Automatic Cup-to-Disc Ratio Estimation Using Active Contours and Color Clustering in Fundus Images for Glaucoma Diagnosis

Irene Fondón[1], Francisco Núñez[1], Mercedes Tirado[1], Soledad Jiménez[2], Pedro Alemany[3], Qaisar Abbas[4], Carmen Serrano[1], and Begoña Acha[1]

[1] Signal Theory Departament, University of Seville, Seville, Spain
irenef@us.es, {kinube,mertirpen}@gmail.com,
{cserrano,bacha}@us.es
[2] Hospital Universitario Puerta del Mar, Cádiz, Spain
soledad.jimenez@ono.com
[3] Surgery Department, University of Cádiz, Cádiz, Spain
pedromaria.alemany@uca.es
[4] Department of Computer Science, National Textile University, Faisalabad, Pakistan
drqaisar@ntu.edu.pk

Abstract. In this paper we propose a new automatic technique for the segmentation of the Optic Disc (*OD*) and optic nerve head (cup) regions in retinographies for glaucoma diagnosis. It provides an estimation of the Cup-to-Disc Ratio, the main clinical indicator of the disease. *OD* is detected combining intensity-based, multi-tolerance and morphological methods along with the active contour technique. Cup region is obtained with a new human perception adapted version of the well-known *K*-means algorithm in the uniform *CIE* $L^*a^*b^*$ color space with *CIE94* color difference. For comparisons, the accurate cup border obtained is rounded and soften with two different techniques: ellipse fitting and mathematical morphology along with Gaussian Smoothing. The proposed method with both rounding steps has been tested in a database of 55 images and compared with the ground truth provided by an expert ophthalmologist. Both, *OD* and cup region, were satisfactory localized, achieving a mean error of 0.14 for ellipse fitting and 0.13 for morphology. The algorithm proposed seems to be a robust and reliable tool worthy to be included in any *CAD* system for glaucoma screening programs.

Keywords: glaucoma, cup-to-disc-ratio, retinal images, *K*-means.

1 Introduction

The term glaucoma refers to a large number of diseases affecting the optic nerve. According to the literature [1], [2], glaucoma is the second leading cause of blindness in the world. Although glaucoma causes irreparable damages, its progression may be limited if detected early. In this sense, the optic cup-to-disc ratio (*CDR*) is one of its clinical indicators and, nowadays, it is manually estimated by ophthalmologists.

A. Campilho and M. Kamel (Eds.): ICIAR 2012, Part II, LNCS 7325, pp. 390–399, 2012.

Therefore, mass screening programs are very expensive and time-consuming tasks. Besides, as it has been proved [3], [4], manual estimation of the *CDR* is highly dependent on the experience and skill of the clinicians. Hence, the use of a fully-automatic and robust *CAD* tool seems to be necessary. Image processing approaches to *CDR* estimation include an initial segmentation phase where the *OD* and cup are isolated from the background in retinal fundus images. To accomplish this objective, many different approaches have been developed in the past [5]-[7] with a variety of results, but none of them have obtained a complete success. Therefore, the problem remains unsolved yet. None of the state of the art methods make use of full color information, only taking into account one color plane or the gray level representation of the original image. Subsequently, they are based on the intensity values of the images under test. In this paper we propose a novel technique that tries to take advantage of the color information that characterized the cup inside the *OD* area. After *OD* area is obtained through an active contour method, a color clustering technique adapted to human perception is carried out to detect the cup area inside the *OD*.

2 Algorithm Description

The algorithm processes the image, following the steps shown in Fig. 1. The first stage is the segmentation and extraction of blood vessels. It has been performed with an adaptive surface-based segmentation method [8]. The *OD* center is localized with a hybrid technique based on anisotropic diffusion [9] and intensity variation [5]. Then, a localized region-based active contour method [10] is applied to get a first estimation of the *OD*. This rough boundary is processed with a multitolerance morphological area opening to obtain the final *OD*. Once the *OD* region is defined, an unsupervised pixel clustering method based on *CIE94* color distance is performed, where the number of labeled clusters is automatically selected through the maximization of Dunn coefficient [11]. According to this, a first cup estimation is obtained by selecting the set of pixels with the brightest yellow color. Many state of the art algorithms provide a round and smooth cup boundary as their final results. Subsequently, a rounded version of the so obtained cup boundary is finally built with two different methods: fitting a least square ellipse, which is the most extended technique in the literature, and a novel approach proposed in this article based on a gaussian smoothing of the cup boundary that results after dilating the primary set of pixels.

2.1 Vascular Tree Segmentation

The blood vessel extraction step is performed in the green channel of the original image. As it is addressed on Fig. 2, this channel is preprocessed by means of a polynomial contrast enhancement method proposed by Walter et al. [12] which has been slightly modified to achieve a better accuracy [8]. Then, the top-hat version of

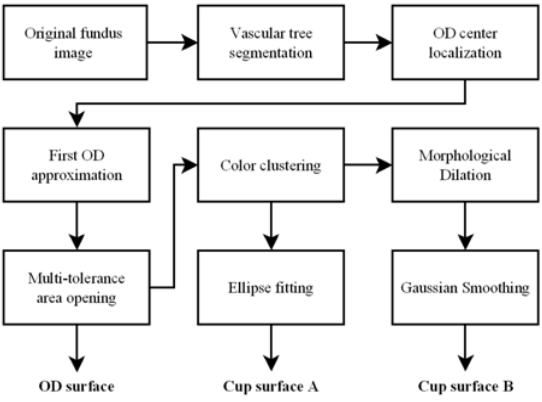

Fig. 1. Flow chart of the proposed method

the high-pass filtered image is calculated and subtracted from the contrast enhanced image. Afterwards, an adaptive surface-based threshold is applied to this image in order to obtain a vascular tree with an area of nearly 10.5% of the total area of the image. This empirically obtained value is independent on the image quality.

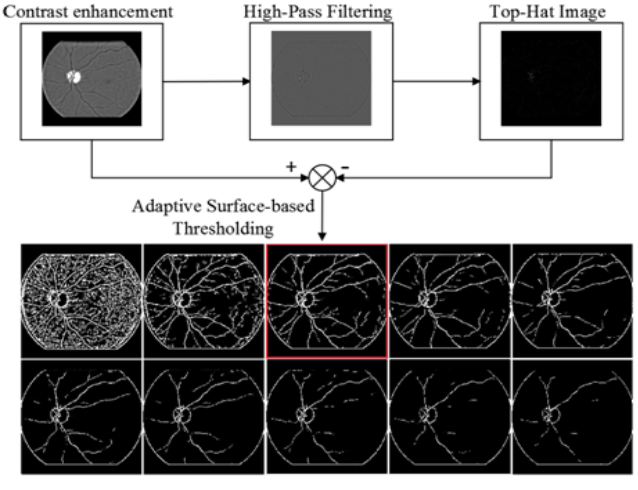

Fig. 2. Vascular tree segmentation process. The highlighted image is the final segmented tree.

2.2 *OD* Center Localization

Once the blood vessels have been segmented, we make use of the green channel of the original image, Fig. 3 (a), to find the *OD* center following a method based on the work proposed by Sinthanayothin et al.[5]. Due to the presence in the *OD* region of dark blood vessels and bright cup area, its intensity variation must be the highest of the image. A practical translation of this observed characteristic is the computation of the variance of

the image. As the variance is a contrast measure, it gives an approximated idea of its homogeneity, having high values for those pixels with a high difference with their neighbors. Only two areas of the retinography are then supposed to have high variance levels: the *OD* and the eye edges. In order to discard false centers outside the *OD* belonging to these eye edges a binary mask is built by blurring the green channel of the image with an anisotropic diffusion filter [9], Fig. 3 (b), and subsequently thresholding the blurred image, Fig. 3 (c) . As pixels belonging to the *OD* will have high intensity levels, the threshold is fixed to the maximum of the blurred image ponderated to the 90%. Typically it achieves values between 0,5 and 0.65.

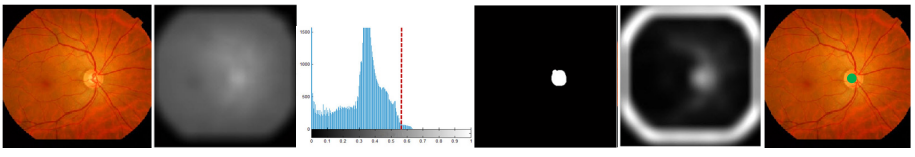

(a) **(b)** **(c)** **(d)** **(e)** **(f)**

Fig. 3. Green channel of image (a) is blurred (b) and thresholded (c). The final binary mask is shown in (d). (e) mean variance computed on the green channel. The *OD* area and the edges of the eye are the only highlighted areas. (f) Final *OD* center marked in green.

Next, we compute the variance of the green channel image using windows of 21x21 pixels, Fig. 3 (e). Finally, the center of the *OD* is the pixel with the highest average variance within the group of pixels that belongs to the mask. The final result is shown in Fig. 3 (f).

2.3 First OD Approximation

Before *OD* region could be identified, the detected blood vessels must be removed. This is performed by applying to the red plane of the image a slighted modified anisotropic diffusion operation [5] that assigns different diffusion coefficients regarding on the pixel position. The objective is to smooth inside the regions limited by edges but not through them. Subsequently we delete non necessary information as the little and thin capillaries, hemorrhages and mycroaneurisms while preserving the *OD* contour. Afterwards, a localized region-based active contour process can be initialized [10]. The initial boundary is a 100 pixels side length square box centered in the *OD* center. In this way, it is assured that the *OD* boundary is, at least, partially contained inside the initial contour. In order to achieve a good accuracy, two parameters must be managed: the localization radius and the number of iterations. The first one must be set according to the size and shape of the object to be segmented. As we are looking for the *OD* boundary, we assume a pseudo-elliptical form with a localization radius empirically set to 20 pixels. The number of iterations is strongly dependent on the image size, initial contour size and location respect to the *OD*. Based on our conditions, this value has been set to 120 in order to not under-segment any image. When this method is applied, a generally coarse and noisy *OD* boundary is obtained and, occasionally, over-segmentation occurred. The procedure is illustrated in Fig. 4.

2.4 Multi-tolerance Area Opening

At this point we have a curve which defines a coarse *OD* boundary. In order to obtain an accurate boundary we make use of morphological techniques, specifically the area opening operation. In our case, the best fitting shape of the structuring element is a disc, due to the generic shape of the *OD*. The choice of a suitable disc size may become a critical issue in the *OD* surface extraction process. In order to overcome this issue and achieve high accuracy, a multi-tolerance area opening method has been developed, where the disc size is automatically estimated based on the coarse *OD* boundary stretch. An initial value for the disc radius is assigned according to our database average *OD* radius size. If after the area opening a null result is obtained, which implies that the disc does not fit into the coarse *OD* boundary, the radius is recalculated. This process is repeated as many times as necessary to obtain a positive result after the area opening. Its value is obtained following the next expression:

$$r_i = \left\lfloor \frac{1}{k_i}\sqrt{\frac{S_{res}}{7\pi}} \right\rfloor, \quad k_{i+1} = k_i + \Delta,\ i = 0,1,\ldots,N-1 \tag{1}$$

where r_i is the disc radius at the iteration i, S_{ret} is the retinal area taken as the image resolution in pixels, k_i is the scaling factor in the iteration i, Δ is an incremental factor and N is the number of iterations. This formula is based on the physiological evidence that the *OD* radius is approximately 1/7 of the retinal radius, and its parameters have been set empirically to k_0=3 and Δ=0.1. The result of this operation is the final *OD* area, which will be used for the *CDR* estimation in the final step of the process. An example of this stage is shown in Fig. 4.

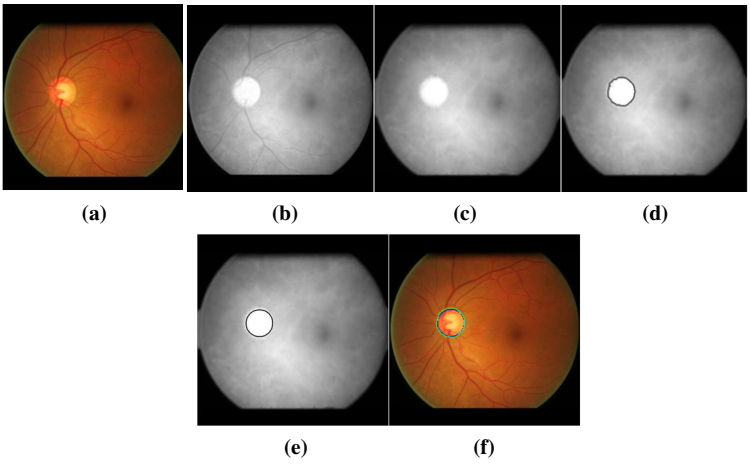

Fig. 4. Red channel of the original image (a), image (b), is processed to remove vessels with an anisotropic diffusion filter (c). A coarse *OD* boundary is obtained after active contours segmentation (d). (e) represents the final *OD* area after multi-tolerance area opening superimposed to (b). In (f) the coarse (green) and final (blue) *OD* boundary are outlined over (a) image.

2.5 Color Clustering

Once the *OD* area has been isolated, the cup region can be identified within it. State of the art methods address this issue by processing the image with gray level techniques such as level set or thresholding [13]. As far as our knowledge, none of the published articles had paid any attention to the color information present in the retinography. Therefore, in this paper we propose to take advantage of the a priori knowledge about color distribution in the *OD* area. Blood vessels have a dark reddish color. There is also a little portion of background in different shades of orange, and above all, the cup area is characterized by its high level of brightness that makes it to appear nearly yellow, as can be seen in Fig. 5. Therefore, a segmentation method based on color information could identify the cup area from the rest of elements by searching for the brightest yellow pixels within the *OD*. Stated this, and in order to perform the color segmentation, a uniform color space is required. That is, in the chosen color space, distance measures must be correlated with perceived color differences. In 1976, *CIE* proposed two color spaces that approximately possessed this property: *CIE* $L^*a^*b^*$ and *CIE* $L^*u^*v^*$. Euclidean distances in those spaces were believed to be approximately correlated with perceptual color differences. Later on, it was shown that this goal was not strictly achieved. To improve the uniformity of color difference measurements in *CIE* $L^*a^*b^*$, *CIE94* an empirical modification of the Euclidean distance was proposed in 1995 [14]. More recently, the *CIE* has established the *CIEDE2000* color difference equation [15] that extends the concept of *CIE94* with further complexity. *CIE94* and *CIEDE2000*, are almost identical and therefore, to avoid an increase on computational complexity, *CIE94* is the preferred metric. As cup area is distinguishable from the rest of the *OD* elements, *CIE94* can provide the human related results needed with the less amount of computational cost. Once the color space and the distance metric are chosen, the segmentation algorithm that would partition the data space must also be selected. In this approach, due to its simplicity and effectiveness we have chosen a method based in the well-known *K*-means clustering technique adapted it to human perception. This clustering procedure can be summarized as follows. Let $X = \{x_1, \ldots, x_n\}$ be the pixels contained in the *OD* area represented in the $L^*a^*b^*$ color space. The codebook V is defined as the set $V = \{v_1, \ldots, v_k\}$, whose elements are the centroids of the colors present in the region under study, in our case *OD* area. The Voronoi set π_i of the codevector v_i is the subset of X for which the centroid v_i is the nearest vector. Starting from the finite data set X, this algorithm moves iteratively the k codevectors to the centroids of their Voronoi sets and recalculates the Voronoi sets. The codebook V is chosen to minimize the empirical quantization error:

$$E(V) = \frac{1}{2n} \sum_{i=1}^{K} \sum_{x \in \pi_i} d^2(x, v_i) \tag{2}$$

where d is the distance measure, usually Euclidean, and n the number of pixels. However, as we have already mentioned, Euclidean distance cannot correct the non-uniformity present in the color space, leading to undesirable results. To overcome this problem, while adapting the algorithm to human perception, with the lowest increment in complexity, we have modified this *K*-means algorithm to work with the advanced *CIE94*

metric. Due to space restrictions, the authors recommend the interested reader reference [14] for a complete description of this advance color difference formula. In this context, the codebook for *K*-means algorithm implementation, chosen to minimize the empirical quantization error, can be obtained through an optimization process looking for the minimum of eq. 2 with *d* as the *CIE94* color distance. This optimization procedure is performed in the case of the Euclidean distance by computing the first derivative of the distance equation an equaling it to zero. Unfortunately, due to the nature of the *CIE94* color distance formula, the same method cannot be used with this advanced metric because it leads to an equation system extremely difficult to solve. Consequently, a heuristic method based on the direction of the gradient vector has been adopted in the proposed approach. At each image pixel, the gradient vector points in the direction of largest possible function increase, corresponding its magnitude to the rate of change in that direction. The opposite one corresponds, then, to the direction of the function decrease and therefore it can be used to obtain its local minima. Hence, to find the location of the new codevectors, the algorithm moves from the old centroids in the opposite direction to the gradient. When moving along this direction, the function value will decrease until a local minimum is reached. In that particular moment, if the algorithm keeps moving, the function will increase. This growing in the function's value is an indicator of the approximate location of the new codevector. As a result of this *K*-means procedure, every pixel in the *OD* area is assigned to one of the color centroids. To identify the cup group, the algorithm compares the mean lightness of each of the clusters, choosing the one with the highest value. A clustering result can be observed in Fig. 5.

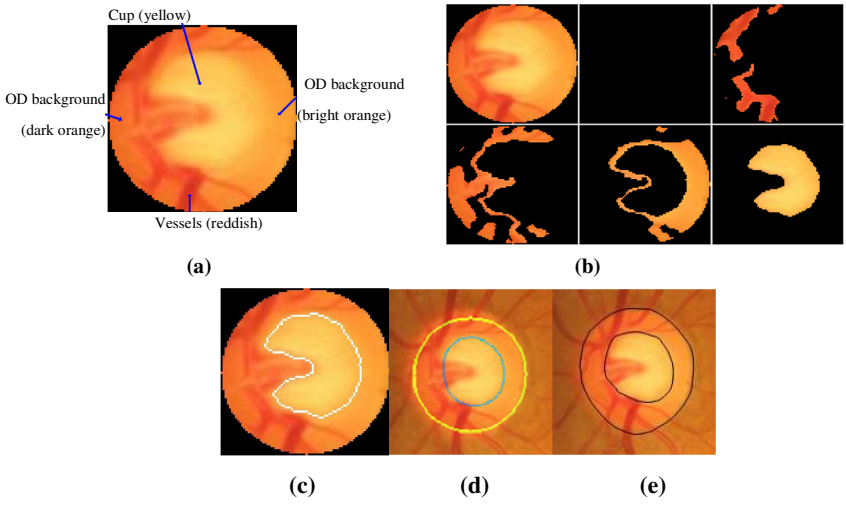

Fig. 5. (a) Cup color distribution. (b) Color groups obtained after *K*-means procedure. (c) Final cup region superimposed on the detected *OD* area. (d) final *OD* (yellow) and cup (blue) boundaries. (e) *OD* and cup manually segmented.

2.6 Looking for an Smooth Round Area

Although the obtained cup boundary is accurate, some experts prefer a round area instead. In the literature many techniques carry out the final cup boundary searching for circles or fitting ellipses [13]. Therefore, an ellipse fitting stage could be

optionally added to our algorithm. To this purpose and once we have extracted the set of pixels classified as cup, an approximately round estimation of the boundary is obtained as the best fitting least square ellipse. The area enclosed within the ellipse will be considered as the cup surface when the *CDR* is calculated by means of this method. We also make use of a morphological dilation technique, with a disc of size 8 pixels as the structuring element, in order to obtain a dilated cup boundary. Since the dilated cup boundary does not fit with the real one a Gaussian smoothing of the boundary is performed with the method described in [16]. It is based on the classic curvature scale-space filtering idea. Finally, the cup surface is the number of pixels enclosed by the so obtained curve. See Fig. 5 (d).

2.7 *CDR* Estimation

Once the *OD* and cup surfaces have been estimated, the *CDR* is obtained as $CDR = \frac{S_{cup}}{S_{OD}}$, where S_{cup} is the cup surface, regardless which rounding method has been adopted, and S_{OD} is the *OD* surface calculated as the number of pixels enclosed by the *OD* boundary.

3 Results

This new technique has been tested in a dataset of 55 which includes healthy, glaucoma suspicious and glaucomatous fundus images, and also images with sharpen, progressive slope, small or blurred cup excavations. All of them were manually segmented by an expert ophthalmologist that marked *OD* and cup boundaries, see Fig. 5 (e). *CDR* has been calculated for these images integrating our ground truth criteria. The *OD* was successfully localized in the 55 images. In 6 images noticeable over-segmentation occurred when the *OD* final boundary was extracted due to high saturation in the red channel. In the remaining images, an accurate segmentation of the *OD* boundary has been achieved. In order to evaluate the goodness of the method, two statistical measures have been calculated:

$$\mu\left(E^{k}\right) = \frac{1}{N}\sum_{i=1}^{N} E_i^k \tag{3}$$

$$\sigma\left(E^{k}\right) = \sqrt{\frac{1}{N}\sum_{i=1}^{N}\left(E_i^k - \mu\left(E^{k}\right)\right)^2},\ k = 1,2 \tag{4}$$

$$E_i^k = \left|CDR_i^k - CDR_i^{GS}\right|,\ i = 1,2,\ldots,N \tag{5}$$

where N is the number of images, CDR_i^{GS} is the *CDR* manually obtained by the expert ophthalmologist in the image i, *GS* stands for Gold Standard, k=1 refers to the first rounding method (fitting the least square ellipse), and k=2 refers to the second one (Gaussian smoothing of the dilated cup boundary). $\mu(E^k)$is the average error and $\sigma(E^k)$ is the standard deviation of the error. In order to obtain these measures, the error E_i^k has been estimated for both cases in every image of the database. In the next table the results for both methods are shown:

Table 1. Mean error and standard deviation of the estimated error for both methods

	Ellipse Fitting Method (*k=1*)	Proposed Method (*k=2*)
$\mu(E^k)$	0,1400	0,1287
$\sigma(E^k)$	0,1166	0,1006

Table 2 shows the obtained results after classifying the error regarding to the intra-observer variability tolerance, to the inter-observer variability tolerance and out of the tolerance limit. With the traditional method we obtain 39 images (70.91% from the whole set) under the inter-observer limit, whereas with the proposed method we obtain a correct diagnosis in 43 images (78.18% of the total set). We can also notice an slight improvement obtained with the proposed method if we take the intra observer limit as the reference because 35 images (63.64%) are correctly classified while the traditional methods provides 34 images under the tolerance limit.

Table 2. Classification of error E in ellipse fitting approach (E^1) and Gaussian smoothing approach (E^2)

	Intra-observer variability (<0,15 CDR units)	Inter-observer variability (<0,2 CDR units)	Out of limit (>0,2 CDR units)
E^1	34 (61,82 %)	39 (70,91 %)	16 (29,09 %)
E^2	35 (63,64 %)	43 (78,18 %)	12 (21,82 %)

According to the results obtained, the second rounding method proposed in this paper for *CDR* estimation improves the accuracy carried out by the least square ellipse fitting traditional approach. Global results are in concordance with the so obtained by other authors in the state of the art literature [13].

4 Conclusions

A novel approach for *CDR* estimation for glaucoma diagnosis has been introduced in this paper. According to the results obtained for a database of 55 images, the method proposed is presented as a feasible alternative in computer-aided glaucoma diagnosis. This work deals with a novel concept in automatic *CDR* estimation techniques: the use of *CIE94* color distance. As we described earlier, this color distance adds a more realistic perceptual color model than the Euclidean color distance, and the three *CIE* $L^*a^*b^*$ color channels are involved in its calculation. Therefore, real color information is taken into account making use of grayscale channels information only for *OD* localization. Besides, with the results endorsement, a new and challenging field is presented when dealing with computer-aided glaucoma diagnosis.

Acknowledgements. The completion of this research was made possible thanks to the projects PI07/90373 and TEC2010-21619-C04-02.

References

1. Resnikoff, S., Pascolini, D., Etya'ale, D., Kocur, I., Pararajasegaram, R., Pokharel, G., Mariotti, S.: Global Data on Visual Impairment in the Year 2002. Bulletin of the World Health Organization 82(11), 887–888 (2004)
2. Quigley, H.A., Broman, A.T.: The Number of People with Glaucoma Worldwide in 2010 and 2020. Br. J. Ophthalmol. 90(3), 262–267 (2006)
3. Watkins, R., Panchal, L., Uddin, J., Gunvant, P.: Vertical Cup-to-Disc Ratio:Agreement between Direct Ophthalmoscopic Estimation, Fundus Biomicroscopic Estimation, and Scanning Laser Ophthalmoscopic Measurement. Optometry and Vision Science 80(6), 454–459 (2003)
4. Varma, R., Spaeth, G.L., Steinmann, W.C., Katz, L.J.: Agreement between Clinicians and an Image Analyzer in Estimating Cup-to-Disc Ratios. Arch. Opthalmol. 107(4), 526–529 (1989)
5. Sinthanayothin, C., Boyce, J.A., Cook, H.L., Williamson, T.H.: Automated Localization of the Optic Disc, Fovea, and Retinal Blood Vessels from Digital Colour Fundus Images. Br. J. Ophthalmol. 83(8), 902–910 (1999)
6. Walter, T., Klein, J.-C.: Segmentation of Color Fundus Images of the Human Retina: Detection of the Optic Disc and the Vascular Tree Using Morphological Techniques. In: Crespo, J.L., Maojo, V., Martin, F. (eds.) ISMDA 2001. LNCS, vol. 2199, pp. 282–287. Springer, Heidelberg (2001)
7. Muramatsu, C., Nakagawa, T., Sawada, A., Hatanaka, Y., Hara, T., Yamamoto, T., Fujita, H.: Automated Segmentation of Optic Disc Region on Retinal Fundus Photographs: Comparison of Contour Modeling and Pixel Classification Methods. Computer Methods and Programs in Biomedicine, 23–32 (2010)
8. Jiménez, S., Alemany, P., Núñez, F., Fondón, I., Serrano, M.C., Acha, B.: A New Method for Automated CDR Measurements in Photographic Retinal Images. In: European Glaucoma Society Congress, vol. 9 (2010)
9. Perona, P., Malik, J.: Scale Space and Edge Detection Using Anisotropic Diffusion. IEEE Transactions on Pattern Recognition and Machine Intelligence 12(7), 629–639 (1990)
10. Lankton, S., Tannenbaum, A.: Localizing Region-Based Active Contours. IEEE Trans. Image Process. 17(11), 2029–2039 (2008)
11. Maulik, S., Bandyopadhyay, S.: Scale-space and edge detection using anisotropic diffusion. IEEE Trans. on Pattern Analysis and Machine Intelligence 24(12), 1650–1654 (2002)
12. Walter, T., Massin, P., Erginay, A., Ordoñez, R., Jeulin, C., Klein, J.C.: Automatic Detection of Microaneurysms in Color Fundus Images. Medical Image Analysis 11(6), 555–566 (2007)
13. Wong, D.W.K., Liu, J., Lim, J.H., et al.: Intelligent Fusion of Cup-to-Disc Ratio Determination Methods for Glaucoma Detection in ARGALI. IEEE Engineering in Medicine and Biology Society: Engineering the Future of Biomedicine 5332534, 5777–5780 (2009)
14. McDonald, R., Smith, K.J.: CIE94 - A New Colour-Difference Formula. J. Soc. Dyers. Col. 111, 376–379 (1995)
15. Luo, M.R., Cui, G., Rigg, B.: The Development of the CIE 2000 Colour-Difference Formula: CIEDE2000. Color Research & Application 26(5), 340–350 (2001)
16. Lee, T.K., McLean, D.I., Atkins, M.S.: Irregularity Index: A New Border Irregularity Measure for Cutaneous Melanocytic Lesions. Medical Image Analysis 7(1), 47–64 (2003)